

## Three-dimensional and temperature-dependent electronic structure of the heavy-fermion compound $\text{CePt}_2\text{In}_7$ studied by angle-resolved photoemission spectroscopy

Yang Luo,<sup>1</sup> Chen Zhang,<sup>1</sup> Qi-Yi Wu,<sup>1</sup> Fan-Ying Wu,<sup>1</sup> Jiao-Jiao Song,<sup>1</sup> W. Xia,<sup>2,3</sup> Yanfeng Guo,<sup>2,3</sup> Ján Ruzsák,<sup>4</sup> Peter M. Oppeneer,<sup>4</sup> Tomasz Durakiewicz,<sup>5</sup> Yin-Zou Zhao,<sup>1</sup> Hao Liu,<sup>1</sup> Shuang-Xing Zhu,<sup>1</sup> Ya-Hua Yuan,<sup>1</sup> Xiao-Fang Tang,<sup>1</sup> Jun He,<sup>1</sup> Shi-Yong Tan,<sup>6</sup> Y. B. Huang,<sup>7</sup> Zhe Sun,<sup>8</sup> Yi Liu,<sup>8</sup> H. Y. Liu,<sup>9</sup> Yu-Xia Duan,<sup>1</sup> and Jian-Qiao Meng<sup>1,10,\*</sup>

<sup>1</sup>*School of Physics and Electronics, Central South University, Changsha 410083, Hunan, People's Republic of China*

<sup>2</sup>*School of Physical Science and Technology, ShanghaiTech University, Shanghai 201210, People's Republic of China*

<sup>3</sup>*School of Physical Sciences, University of Chinese Academy of Sciences, Beijing 100049, China*

<sup>4</sup>*Department of Physics and Astronomy, Uppsala University, Box 516, S-75120 Uppsala, Sweden*

<sup>5</sup>*Institute of Physics, Maria Curie Skłodowska University, 20-031 Lublin, Poland*

<sup>6</sup>*Science and Technology on Surface Physics and Chemistry Laboratory, Mianyang 621908, People's Republic of China*

<sup>7</sup>*Shanghai Institute of Applied Physics, CAS, Shanghai 201204, People's Republic of China*

<sup>8</sup>*National Synchrotron Radiation Laboratory, University of Science and Technology of China, Hefei 230029, Anhui, People's Republic of China*

<sup>9</sup>*Beijing Academy of Quantum Information Sciences, Beijing 100085, People's Republic of China*

<sup>10</sup>*Synergetic Innovation Center for Quantum Effects and Applications (SICQEA), Hunan Normal University, Changsha 410081, People's Republic of China*



(Received 24 October 2019; revised manuscript received 29 February 2020; accepted 2 March 2020; published 18 March 2020)

The three-dimensional and temperature-dependent electronic structures of the heavy-fermion superconductor  $\text{CePt}_2\text{In}_7$  are investigated. Angle-resolved photoemission spectroscopy using variable photon energy establishes the existence of quasi-two- and three-dimensional Fermi surface topologies. Temperature-dependent  $4d$ - $4f$  on-resonance photoemission spectroscopies data reveal that heavy quasiparticle bands begin to form at a temperature well above the characteristic (coherence) temperature  $T^*$ . The emergence of low-lying crystal electric field excitation may be responsible for the “relocalization” or the precursor to the establishment of heavy electrons coherence in heavy-fermion compounds. These findings provide critical insight into understanding the hybridization in heavy-fermion systems.

DOI: [10.1103/PhysRevB.101.115129](https://doi.org/10.1103/PhysRevB.101.115129)

### I. INTRODUCTION

Heavy fermions (HFs) have long been the focus of condensed matter physics because of their rich and exciting physical phenomena [1,2], including quantum criticality, magnetic order, and unconventional superconductivity coexistence, and non-Fermi-liquid behaviors. This system's diverse and tunable ground states result in various materials types, such as HF superconductors, Kondo insulators, and HF antiferromagnetism (AFM) or ferromagnetism. HFs ground state can be easily tuned using pressure, magnetic field, and doping [3].

A characteristic temperature,  $T^*$ , for HF materials, called “hybridization temperature” or “coherent temperature” is defined. There are different views on the physics which underlies  $T^*$  and what determines it.  $T^*$  is currently believed to be collective hybridization onset between localized  $f$  electrons and conduction electrons [4], leading to the emergence of heavy electrons at lower temperatures [5,6]. Several techniques are available to determine  $T^*$ , including thermodynamics, transport, Knight shift measurements [7], nuclear magnetic resonance (NMR) [8], and inelastic neutron scattering (INS) [9].

A question that remains is whether any  $T^*$  determined by various techniques or researchers using the same techniques has the same underlying physics. INS studies have revealed that the characteristic temperature  $T^*$  of  $\text{CeMIn}_5$  is tens of kelvin [9]. Angle-resolved photoemission spectroscopy (ARPES) studies have found that heavy quasiparticle bands begin to form well above  $T^*$ , and show a crossover behavior across  $T^*$  [10–13]. A laser-based ARPES study of  $\text{YbRh}_2\text{Si}_2$  showed that coherent states developed just below  $T^*$  [14]. Knowing what determines  $T^*$  is of fundamental and practical importance and is a prerequisite for understanding HF physics.

We chose the AFM HF superconductor  $\text{CePt}_2\text{In}_7$  to study this concern.  $\text{CePt}_2\text{In}_7$ , discovered in 2008 [15], is a member of a widely studied HF compound family  $\text{Ce}_m\text{M}_n\text{In}_{3m+2n}$  ( $M = \text{Co, Rh, Ir, Pt}$ ) [10–13,16–23]. At ambient pressure,  $\text{CePt}_2\text{In}_7$  undergoes an AFM phase transition at the Néel temperature  $T_N = 5.2$  K [24]. Under pressure,  $\text{CePt}_2\text{In}_7$  has a bulk superconducting transition temperature of up to  $T_c = 2.1$  K (near 3.5 GPa [25]). AFM and superconductivity exist simultaneously within a certain pressure range [25–27]. Nuclear quadrupolar resonance and muon spin rotation/relaxation data revealed commensurate [28,29], or coexisting commensurate and incommensurate [8,30], AFM orders. Quantum oscillation [31,32] and ARPES

\*Corresponding author: [jqmeng@csu.edu.cn](mailto:jqmeng@csu.edu.cn)

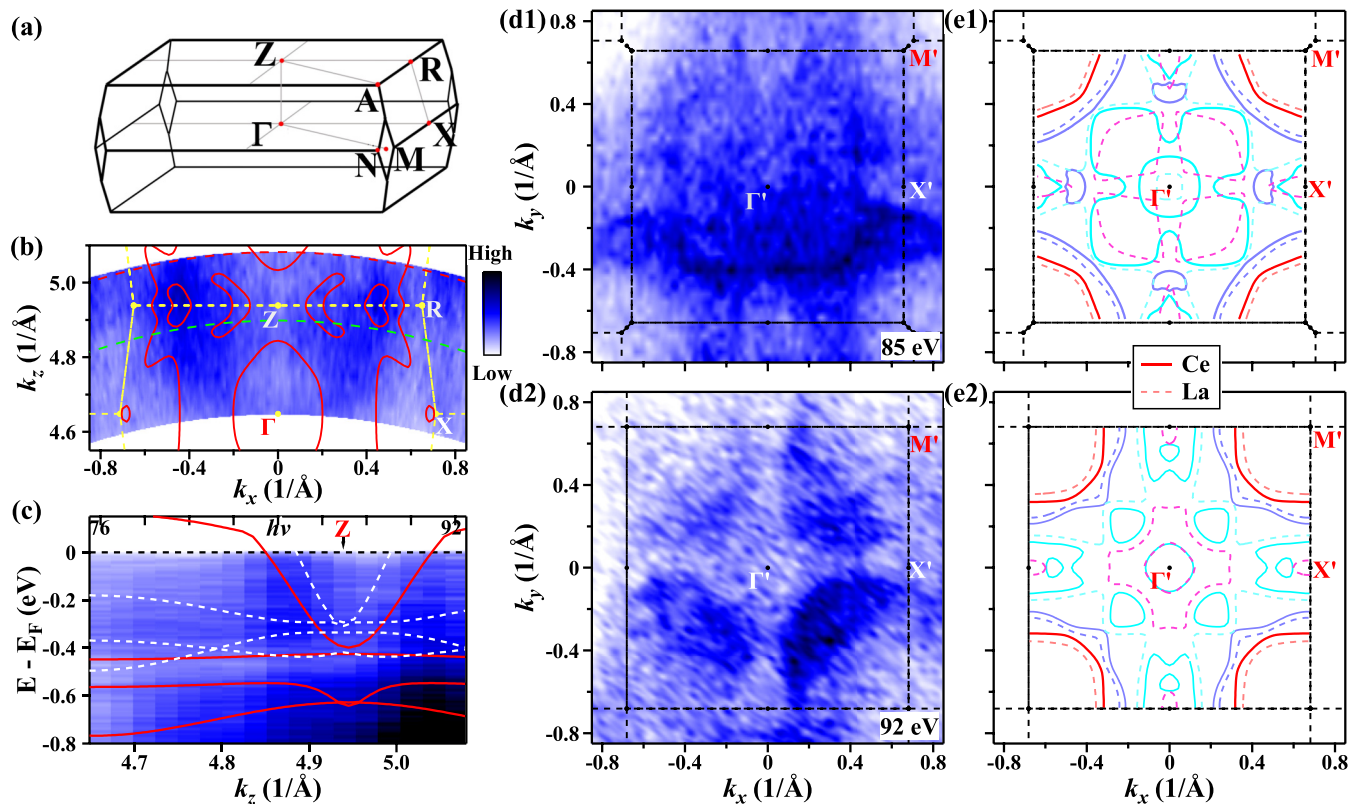


FIG. 1. CePt<sub>2</sub>In<sub>7</sub> FS at low temperature. (a) A 3D Brillouin zone (BZ) of CePt<sub>2</sub>In<sub>7</sub> with high-symmetry momentum points (red dots) marked. (b) Experimental 3D FS maps measured using  $h\nu = 76\text{--}92$  eV photons in 1 eV steps, in the  $\Gamma$ ZRX plane. (c)  $k_z$  dispersion along the  $\Gamma$ -Z- $\Gamma$  high-symmetry direction, obtained by varying  $h\nu$  from 76 to 92 eV. The calculated band structures of CePt<sub>2</sub>In<sub>7</sub> (solid red lines) and LaPt<sub>2</sub>In<sub>7</sub> (white-dashed lines) were overlaid. (d1),(d2) Spectral weight as a function of 2D momentum ( $k_x, k_y$ ) taken with 85 and 92 eV photons, respectively. Momentum cuts with 85 and 92 eV photons are marked with green and red lines, respectively, in (b). All photoemission intensity data were integrated over an  $[-20\text{ meV}, 20\text{ meV}]$  energy window with respect to the Fermi energy  $E_F$ . (e1),(e2) The corresponding calculation results in (d). Solid and dashed lines represent the results for CePt<sub>2</sub>In<sub>7</sub> and LaPt<sub>2</sub>In<sub>7</sub>, respectively. All the calculated results shown here are adapted from Ref. [23].

measurements [23,33] revealed a complex Fermi-surface (FS) topology composed of quasi-two-dimensional (quasi-2D) sheets, or coexisting quasi-2D and three-dimensional (3D) character. Recently, weaker hybridization was revealed by optical spectroscopy [34] and ARPES [23]. NMR determines a  $T^* \sim 20$  K [8]. Knight shift measurements return a  $T^* \sim 40$  K, but exhibit the delocalization at further lower temperatures [7].

## II. EXPERIMENTAL DETAILS

In this study, we varied the temperature between 15 and 135 K above the Néel temperature. CePt<sub>2</sub>In<sub>7</sub> FS topology along the  $k_z$  (perpendicular) direction was mapped out using systematic photon energy dependence ( $h\nu = 76\text{--}92$  eV) and constant photon energy ( $h\nu = 85$  and 92 eV) ARPES measurement. FS measured topology was compared to density-functional theory (DFT) calculations [23]. Ce 4*f* electrons properties were investigated by comparing off- and on-resonance spectra. Temperature-dependent studies showed that below 60 K, crystal electric field (CEF) splitting might result in “relocalization” of the itinerant *f* electrons.

High-quality CePt<sub>2</sub>In<sub>7</sub> single crystals were grown using an In self-flux method. Data presented in Figs. 1(b), 1(c), and 2 were obtained at the “Dreamline” beamline of the Shanghai

Synchrotron Radiation Facility using a Scienta DA30 analyzer, and the vacuum was kept below  $1 \times 10^{-10}$  mbar. Data shown in Figs. 1(d) and 3 were obtained at beamline 5-2 of the Stanford Synchrotron Radiation Lightsource using a Scienta D80 analyzer, with a base pressure of better than  $6 \times 10^{-11}$  mbar. The typical angular resolution was  $\sim 0.2^\circ$ . The overall energy resolution is better than 20 meV. All samples were cleaved *in situ* at  $\sim 15$  K. On-resonance 121/123 eV photons and off-resonance 114 eV photons were used to investigate the nature of Ce 4*f* electrons.

## III. RESULTS AND DISCUSSIONS

3D FS topologies of CePt<sub>2</sub>In<sub>7</sub> were obtained from photon-energy-dependent normal emission at a temperature of 20 K [Fig. 1(b)]. The measurement was performed in a section of the high-symmetry  $\Gamma$ ZRX plane of the CePt<sub>2</sub>In<sub>7</sub> BZ. Different  $k_z$  values were accessed by varying photon energies between 76 and 92 eV. The corresponding  $k_z$  range covers more than half a BZ and included both  $\Gamma$  and Z points. DFT calculated Fermi contours were overlaid on measured intensities. Fermi sheets’ intensity and shapes vary with photon energy. Also, in Fig. 1(c), we observe the clear  $k_z$  dispersion along the  $\Gamma$ -Z- $\Gamma$  line. This demonstrates the 3D character of the electronic

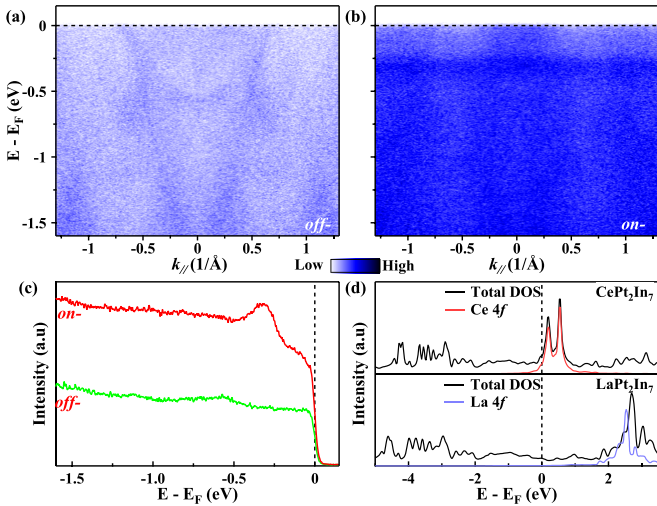


FIG. 2. (a),(b) Off- and on-resonance, respectively, valence band structure of  $\text{CePt}_2\text{In}_7$  at 20 K with 114 eV and 123 eV, measured along the  $X-\Gamma-X$  direction. (c) Angle-integrated photoemission spectroscopy of the intensity plot in (a) and (b). The integrated momentum range is  $[-0.15 \text{ \AA}^{-1}, 0.15 \text{ \AA}^{-1}]$ . (d) Comparison of density of state (DOS) vs energy  $E$  for the isostructural compounds  $\text{CePt}_2\text{In}_7$  (upper panel, adopted from Ref. [23]) and  $\text{LaPt}_2\text{In}_7$  (lower panel).

structure of  $\text{CePt}_2\text{In}_7$  along the  $\Gamma-Z$  direction, consistent with theoretical calculations [23,33,35]. This also clarifies that the incident photons selectively detect the bulk band dispersion. Besides, it can be seen from the figure that the calculated results of  $\text{CePt}_2\text{In}_7$  are more consistent with the experimental results, such as the volume of inner electronlike pocket cen-

tered at the  $Z$  point and the bands at higher binding energy. That means that the Ce  $4f$  electrons are not entirely localized, part of them are itinerant.

Constant photon energy  $k_x-k_y$  FS mappings were taken to clarify FS topological structures. Figures 1(d1) and 1(d2) display the FS intensity maps measured at 18 K with 85 and 92 eV photon energies, respectively. The shape of the  $\Gamma'$  centered FSs change markedly with photon energies, indicating a strong  $k_z$  dependence due to its 3D nature, as shown in Figs. 1(b) and 1(c). In contrast, the shape of electronlike FSs around the  $M'$  point does not change much with incident photon energies, confirming its 2D-like nature. The schematic of the theoretical FS topologies of  $\text{CePt}_2\text{In}_7$  is shown in Figs. 1(e), corresponding to Figs. 1(d). The topology of FS of  $\text{CePt}_2\text{In}_7$  consists of nearly 2D nature FSs near the  $M'$  (zone corner) and strong 3D nature FSs at other momenta. Also, the calculated FS contours for isostructural compounds  $\text{LaPt}_2\text{In}_7$  at corresponding  $k_z$  were overlaid. Comparing Ce and La in Figs. 1(e), we see that the extra  $f$  electron is accommodated by changing the volume of FSs. The two electronlike FSs around the  $M'$  point expand from  $\text{LaPt}_2\text{In}_7$  to  $\text{CePt}_2\text{In}_7$ . And, at other momenta, the shape and size of the FSs change dramatically. The experimental FSs show good agreement with DFT calculations. This may possibly be due to the fact that FSs are contributed by In and Pd characters. Ce  $4f$  electrons may also participate in FS formation, but that contribution is relatively weak. However, due to the diffuse signal near the Fermi energy ( $E_F$ ), it is difficult to distinguish which one is better following the experimental  $k_x-k_y$  FSs.

The  $4d \rightarrow 4f$  on-resonant ARPES measurements were performed with 123 eV photons to strengthen the Ce  $4f$ -electron photoconduction matrix element. Figures 2(a)

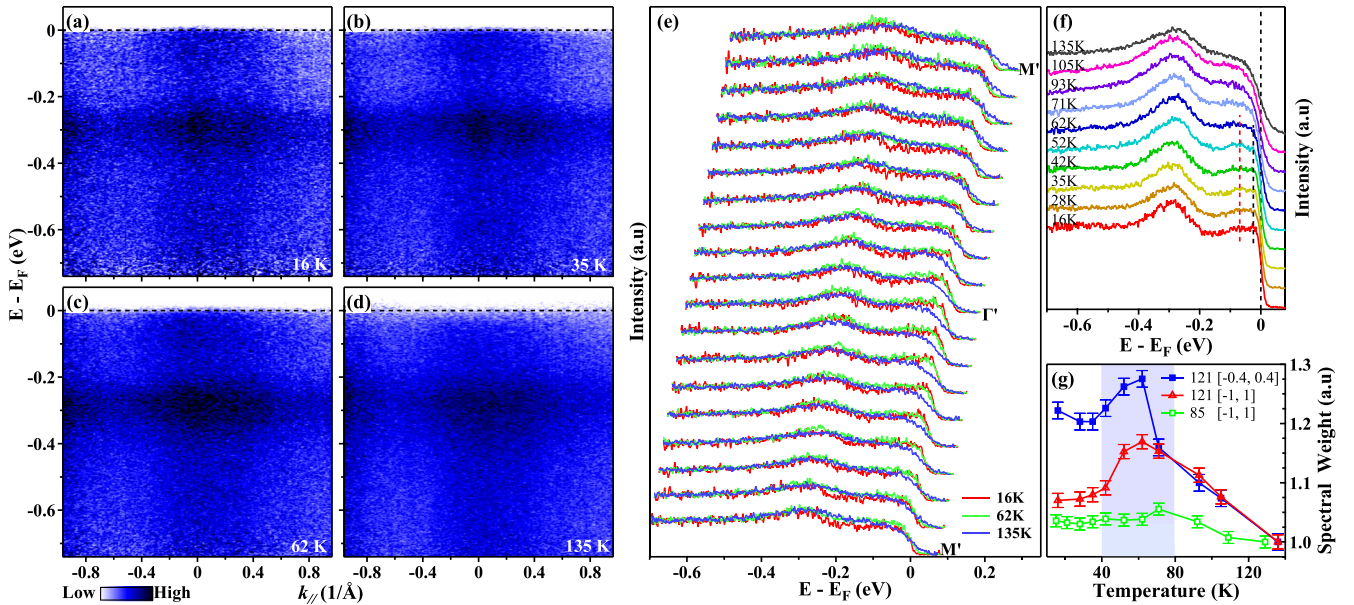


FIG. 3. Temperature evolution of the heavy quasiparticle band. (a)–(d)  $\text{CePt}_2\text{In}_7$  band structure measured along the  $M'-\Gamma'-M'$  direction with 121 eV photons at different temperatures. (e) Detailed ARPES spectra of  $\text{CePt}_2\text{In}_7$  measured at 16, 62, and 135 K. (f) Angle-integrated photoemission spectroscopy at various temperatures. The integrated momentum range is  $[-0.4, 0.4]$ . (g)  $T$  dependence of the quasiparticle spectral weight near  $E_F$ , integrated over  $[E_F - 100 \text{ meV}, E_F + 20 \text{ meV}]$ . The green line represents nonresonant data with 85 eV photons (images not shown here), which measure the DOS with less disturbance. The momentum integral ranges for blue, red, and green lines are  $[-0.04, 0.4]$ ,  $[-1, 1]$ , and  $[-1, 1]$ , respectively. The unit of momentum used here is  $\text{\AA}^{-1}$ .



and 2(b) compare off-resonance with 114 eV photons and on-resonance with 123-eV photons photoemission spectra at 20 K, respectively. The off-resonance spectra are dominated by Pt  $5d$  and In  $5p$  states derived dispersive bands. They show a density of states close to the  $E_F$  of non- $f$  orbital character. The Ce  $4f$  state is enhanced in on-resonance data. The integral spectra in Fig. 2(c) also show this. Two nearly flat bands originate from the spin-orbit splitting of the  $f^1$  final state can be observed in the on-resonance data. This has been seen in prior experiments [23]. The  $\sim 300$  meV is assigned to  $4f_{7/2}^1$ . The other near  $E_F$  is attributed to  $4f_{5/2}^1$  [23]. Similar structures have been observed with other members of the  $Ce_mM_nIn_{3m+2n}$  family [10–13,16–18] and in nonfamily member  $CeCu_2Si_2$  [36].

Figure 2(d) is a comparison of the calculated density of state (DOS) of the isostructural compounds  $CePt_2In_7$  [23] and  $LaPt_2In_7$ . Only the  $4f$  occupation is varied. Compared to the La  $4f$  electrons in  $LaPt_2In_7$  (blue line), which are far away from  $E_F$ , the Ce  $4f$  electrons (red line) are also above  $E_F$ , but some fragments leak below  $E_F$ . The low density of states of the  $4f$  electron below  $E_F$  and the weak  $c$ - $f$  hybridization [23] are responsible for the Ce  $4f$  on-resonance spectrum having only a very slight enhancement, which is not as significant as that observed in the U  $5f$  on-resonance spectrum [37].

The  $f$ -electron properties of HF compounds, localized or itinerant, and how they transform as a function of temperature, have been critical issues in understanding HF physics. Above a characteristic temperature,  $T^*$ ,  $f$  electrons are completely localized. Below  $T^*$ ,  $f$  electrons exhibit a dual nature. They are partially localized and partially itinerant [5,6,38]. Temperature-dependent ARPES measurements on  $CePt_2In_7$  were conducted to better understand how Ce  $4f$ -electron localization and itinerancy evolves with temperature.

Figures 3(a)–3(d) display the temperature-dependent Ce  $4d \rightarrow 4f$  on-resonant ARPES measurements along the  $M'-\Gamma'-M'$  direction with 121 eV photons. Two flat bands with the Ce  $4f$ -electron character exist throughout the measured temperature range. They are weakened at high temperatures. The intensity of the two flat bands is strongly momentum dependent. Figure 3(e) compares EDCs measured at 16, 62, and 135 K. The main structure is similar. The structure near  $E_F$  varies significantly with temperature. Quasiparticle peaks located near  $E_F$  show a strong momentum and temperature dependence. Within a very small energy range very close to  $E_F$ , about 40 meV, the EDC intensity increases as the temperature decreases. Over a slightly larger energy range, such as 100 meV, the EDC intensity evolution is no longer monotonous. Figure 3(f) shows the temperature evolution of the integrated EDCs in the momentum range  $[-1 \text{ \AA}^{-1}, 1 \text{ \AA}^{-1}]$ . The formation of the heavy quasiparticle band begins at a temperature  $T$  much higher than its collective hybridization temperature  $T^*$ , which is 40 [7] or 20 K [8] for  $CePt_2In_7$ . This is consistent with previous observations by other research groups made for other members of the family  $CeMIn_5$  [10–12] and  $Ce_2PdIn_8$  [13].

Figure 3(g) quantitatively shows the  $f$ -electron spectral weight evolution with temperature. Spectral weight has been normalized to the highest temperature data. EDC intensity with different momentum integral widths exhibits similar temperature evolution behavior. These results show that  $f$

electrons spectral weight defined in this energy range has unexpected temperature evolution behavior. As the cooling begins, the  $f$  spectral weight increases as temperature decreases. Then, a relocalization phenomenon occurred, that is, the  $f$  spectral weight decreases with a further reduction in temperature. Similar behavior was found in the 85 eV data set (green line). At a higher temperature range, the temperature evolution behavior of the Ce  $4f$  spectral weight is consistent with those of other research groups, and we all believe that heavy quasiparticle bands have formed at elevated temperatures [10–13]. An inconsistency occurs at low temperatures, where we find that the spectral weight of the Ce  $4f$  electron in  $CePt_2In_7$  decreases with the decrease of temperature, which is different from the previous observation that the spectral weight increases with the decrease of temperature [10–13]. Our results reveal that as the temperature falls,  $f$  electrons transit from localized to more itinerant and back to more localized. Relocalization has been reported in  $CePt_2In_7$  by Knight shift measurement and interpreted as a significant precursor to ordering antiferromagnetically [7]. However, the relocalization temperature, 14 K, determined by Knight shift is much lower than the temperature observed here,  $\sim 60$  K.

Previous ultrafast experiments have reported that photoinduced transient reflectivity varies greatly around 60 K [34]. In-plane resistivity shows a bulge around 40–80 K [39]. Looking closely at the EDCs in Fig. 3(f), as indicated by red and black dashed lines, discloses that CEF splitting becomes observable in the  $4f_{5/2}^1$  band around 60 K. The effect becomes more evident as temperature decreases. It appears that the low-energy CEF splitting and relocalization of  $f$  electrons near the  $E_F$  occurs at the same temperature. At low temperatures, a typical energy scale in a HF system is less than 10 meV. As energy resolution is not good enough and the peak of the low-lying heavy quasiparticle band is not sharp enough, no lowest-lying CEF excitation, less than 10 meV, near  $E_F$  was observed. An earlier ARPES experiment that focused on the low-lying flat band near  $E_F$ , with a binding energy of about 4 meV ( $YbRh_2Si_2$ ) [14], suggests that a coherent state developed below the characteristic temperature,  $T^*$ . INS measurements indicated that the  $4f$  conduction electrons interaction energy scale is comparable to that of low-energy CEF splitting [9,40,41]. The relocalization may be caused by the presence of low-energy CEF excitation. And the occurrence of low-energy CEF excitation may be a precursor to the establishment of heavy-electron coherence in HF compounds.

#### IV. CONCLUSIONS

To summarize, the electronic structure of the HF superconductor  $CePt_2In_7$  was studied by ARPES over a wide temperature range. The results provide clear evidence that (i) FSs have coexistence of quasi-2D and 3D topology, which is consistent with DFT calculations; (ii)  $f$  electrons begin to evolve into the formation of HF states at a temperature much higher than the characteristic temperature  $T^*$ ; and (iii) the emergence of a low-lying heavy quasiparticle band caused by CEF splitting may be the reason for the relocalization or the precursor to the establishment of heavy electrons coherence in HF compounds.

## ACKNOWLEDGMENTS

This work was supported by the National Natural Science Foundation of China (Grants No. 11574402 and No. 11874264), ZDXKFZ (Grant No. XKFZ201703), the Innovation-Driven Plan in Central South University (Grant No. 2016CX032), and the Natural Science Foundation of

Shanghai (Grant No. 17ZR1443300). This work was also supported through the Swedish Research Council (VR) and the Swedish National Infrastructure for Computing (SNIC), for computing time on computer cluster Triolith at the NSC center (Linköping). Some preliminary data were taken at beamline 13U of the National Synchrotron Radiation Laboratory (NSRL).

- [1] P. Gegenwart, Q. Si, and F. Steglich, *Nat. Phys.* **4**, 186 (2008).
- [2] C. Pfleiderer, *Rev. Mod. Phys.* **81**, 1551 (2009).
- [3] J. D. Thompson and Z. Fisk, *J. Phys. Soc. Jpn.* **81**, 011002 (2012).
- [4] Y. P. Liu, Y. J. Zhang, J. J. Dong, H. Lee, Z. X. Wei, W. L. Zhang, C. Y. Chen, H. Q. Yuan, Y.-F. Yang, and J. Qi, *Phys. Rev. Lett.* **124**, 057404 (2020).
- [5] Y. F. Yang, Z. Fisk, H. O. Lee, J. D. Thompson, and D. Pines, *Nature (London)* **454**, 611 (2008).
- [6] Y.-F. Yang, *Rep. Prog. Phys.* **79**, 074501 (2016).
- [7] N. apRoberts-Warren, A. P. Dioguardi, A. C. Shockley, C. H. Lin, J. Crocker, P. Klavins, D. Pines, Y.-F. Yang, and N. J. Curro, *Phys. Rev. B* **83**, 060408(R) (2011).
- [8] H. Sakai, Y. Tokunaga, S. Kambe, H. Lee, V. A. Sidorov, P. H. Tobash, F. Ronning, E. D. Bauer, and J. D. Thompson, *J. Phys.: Conf. Ser.* **391**, 012057 (2012).
- [9] T. Willers, Z. Hu, N. Hollmann, P. O. Korner, J. Gegner, T. Burnus, H. Fujiwara, A. Tanaka, D. Schmitz, H. H. Hsieh, H. J. Lin, C. T. Chen, E. D. Bauer, J. L. Sarrao, E. Goremychkin, M. Koza, L. H. Tjeng, and A. Severing, *Phys. Rev. B* **81**, 195114 (2010).
- [10] Q. Y. Chen, D. F. Xu, X. H. Niu, J. Jiang, R. Peng, H. C. Xu, C. H. P. Wen, Z. F. Ding, K. Huang, L. Shu, Y. J. Zhang, H. Lee, V. N. Strocov, M. Shi, F. Bisti, T. Schmitt, Y. B. Huang, P. Dudin, X. C. Lai, S. Kirchner *et al.*, *Phys. Rev. B* **96**, 045107 (2017).
- [11] Q. Y. Chen, D. F. Xu, X. H. Niu, R. Peng, H. C. Xu, C. H. P. Wen, X. Liu, L. Shu, S. Y. Tan, X. C. Lai, Y. J. Zhang, H. Lee, V. N. Strocov, F. Bisti, P. Dudin, J. X. Zhu, H. Q. Yuan, S. Kirchner, and D. L. Feng, *Phys. Rev. Lett.* **120**, 066403 (2018).
- [12] Q. Y. Chen, C. H. P. Wen, Q. Yao, K. Huang, Z. F. Ding, L. Shu, X. H. Niu, Y. Zhang, X. C. Lai, Y. B. Huang, G. B. Zhang, S. Kirchner, and D. L. Feng, *Phys. Rev. B* **97**, 075149 (2018).
- [13] Q. Yao, D. Kaczorowski, P. Swatek, D. Gnida, C. H. P. Wen, X. H. Niu, R. Peng, H. C. Xu, P. Dudin, S. Kirchner, Q. Y. Chen, D. W. Shen, and D. L. Feng, *Phys. Rev. B* **99**, 081107(R) (2019).
- [14] S. K. Mo, W. S. Lee, F. Schmitt, Y. L. Chen, D. H. Lu, C. Capan, D. J. Kim, Z. Fisk, C. Q. Zhang, Z. Hussain, and Z. X. Shen, *Phys. Rev. B* **85**, 241103(R) (2012).
- [15] Z. M. Kurenbaeva, E. V. Murashova, Y. D. Seropegin, H. Noel, and A. I. Tursina, *Intermetallics* **16**, 979 (2008).
- [16] S. I. Fujimori, T. Okane, J. Okamoto, K. Mamiya, Y. Muramatsu, A. Fujimori, T. Narimura, K. Kobayashi, K. Shimada, H. Namatame, M. Taniguchi, H. Harima, D. Aoki, S. Ikeda, H. Shishido, Y. Tokiwa, Y. Haga, and Y. Onuki, *Physica B* **329-333**, 547 (2003).
- [17] S. I. Fujimori, A. Fujimori, K. Shimada, T. Narimura, K. Kobayashi, H. Namatame, M. Taniguchi, H. Harima, H. Shishido, S. Ikeda, D. Aoki, Y. Tokiwa, Y. Haga, and Y. Onuki, *Phys. Rev. B* **73**, 224517 (2006).
- [18] H. Liu, Y. Xu, Y. Zhong, J. Guan, L. Kong, J. Ma, Y. Huang, Q. Chen, G. Chen, M. Shi, Y.-F. Yang, and H. Ding, *Chin. Phys. Lett.* **36**, 097101 (2019).
- [19] F. Steglich, *J. Magn. Magn. Mater.* **100**, 186 (1991).
- [20] R. Settai, T. Takeuchi, and Y. Onuki, *J. Phys. Soc. Jpn.* **76**, 051003 (2007).
- [21] R. Jiang, D. Mou, C. Liu, X. Zhao, Y. Yao, H. Ryu, C. Petrovic, K.-M. Ho, and A. Kaminski, *Phys. Rev. B* **91**, 165101 (2015).
- [22] S. I. Fujimori, *J. Phys.: Condens. Matter* **28**, 153002 (2016).
- [23] Y.-X. Duan, C. Zhang, J. Ruzs, P. M. Oppeneer, T. Durakiewicz, Y. Sassa, O. Tjernberg, M. Månsson, M. H. Berntsen, F.-Y. Wu, Y.-Z. Zhao, J.-J. Song, Q.-Y. Wu, Y. Luo, E. D. Bauer, J. D. Thompson, and J.-Q. Meng, *Phys. Rev. B* **100**, 085141 (2019).
- [24] P. H. Tobash, F. Ronning, J. D. Thompson, B. L. Scott, P. J. W. Moll, B. Batlogg, and E. D. Bauer, *J. Phys.: Condens. Matter* **24**, 015601 (2012).
- [25] E. D. Bauer, H. O. Lee, V. A. Sidorov, N. Kurita, K. Gofryk, J. X. Zhu, F. Ronning, R. Movshovich, J. D. Thompson, and T. Park, *Phys. Rev. B* **81**, 180507(R) (2010).
- [26] H. Sakai, Y. Tokunaga, S. Kambe, F. Ronning, E. D. Bauer, and J. D. Thompson, *Phys. Rev. Lett.* **112**, 206401 (2014).
- [27] E. D. Bauer, V. A. Sidorov, H. Lee, N. Kurita, F. Ronning, R. Movshovich, and J. D. Thompson, *J. Phys.: Conf. Ser.* **200**, 012011 (2010).
- [28] N. apRoberts-Warren, A. P. Dioguardi, A. C. Shockley, C. H. Lin, J. Crocker, P. Klavins, and N. J. Curro, *Phys. Rev. B* **81**, 180403(R) (2010).
- [29] M. Månsson, K. Prša, Y. Sassa, P. H. Tobash, E. D. Bauer, C. Rusu, D. Andreica, O. Tjernberg, K. Sedlak, M. Grioni, T. Durakiewicz, and J. Sugiyama, *J. Phys.: Conf. Ser.* **551**, 012028 (2014).
- [30] H. Sakai, Y. Tokunaga, S. Kambe, H.-O. Lee, V. A. Sidorov, P. H. Tobash, F. Ronning, E. D. Bauer, and J. D. Thompson, *Phys. Rev. B* **83**, 140408(R) (2011).
- [31] M. M. Altarawneh, N. Harrison, R. D. McDonald, F. F. Balakirev, C. H. Mielke, P. H. Tobash, J. X. Zhu, J. D. Thompson, F. Ronning, and E. D. Bauer, *Phys. Rev. B* **83**, 081103(R) (2011).
- [32] K. Götze, Y. Krupko, J. A. N. Bruin, J. Klotz, R. D. H. Hinlopen, S. Ota, Y. Hirose, H. Harima, R. Settai, A. McCollam, and I. Sheikin, *Phys. Rev. B* **96**, 075138 (2017).
- [33] B. Shen, L. Yu, K. Liu, S. Lyu, X. Jia, E. D. Bauer, J. D. Thompson, Y. Zhang, C. Wang, C. Hu, Y. Ding, X. Sun, Y. Hu, J. Liu, Q. Gao, L. Zhao, G. Liu, Z. Xu, C. Chen, Z. Lu, and X. J. Zhou, *Chin. Phys. B* **26**, 077401 (2017).
- [34] R. Y. Chen, S. J. Zhang, E. D. Bauer, J. D. Thompson, and N. L. Wang, *Phys. Rev. B* **94**, 035161 (2016).

- [35] T. Klimczuk, O. Walter, L. Muchler, J. W. Krizan, F. Kinnart, and R. J. Cava, *J. Phys.: Condens. Matter* **26**, 402201 (2014).
- [36] S. Patil, A. Generalov, M. Guttler, P. Kushwaha, A. Chikina, K. Kummer, T. C. Rodel, A. F. Santander-Syro, N. Caroca-Canales, C. Geibel, S. Danzenbacher, Yu. Kucherenko, C. Laubschat, J. W. Allen, and D. V. Vyalikh, *Nat. Commun.* **7**, 11029 (2016).
- [37] J.-Q. Meng, P. M. Oppeneer, J. A. Mydosh, P. S. Riseborough, K. Gofryk, J. J. Joyce, E. D. Bauer, Y. Li, and T. Durakiewicz, *Phys. Rev. Lett.* **111**, 127002 (2013).
- [38] S. Nakatsuji, D. Pines, and Z. Fisk, *Phys. Rev. Lett.* **92**, 016401 (2004).
- [39] V. A. Sidorov, Xin Lu, T. Park, Hanoh Lee, P. H. Tobash, R. E. Baumbach, F. Ronning, E. D. Bauer, and J. D. Thompson, *Phys. Rev. B* **88**, 020503(R) (2013).
- [40] A. D. Christianson, J. M. Lawrence, P. G. Pagliuso, N. O. Moreno, J. L. Sarrao, J. D. Thompson, P. S. Riseborough, S. Kern, E. A. Goremychkin, and A. H. Lacerda, *Phys. Rev. B* **66**, 193102 (2002).
- [41] A. D. Christianson, E. D. Bauer, J. M. Lawrence, P. S. Riseborough, N. O. Moreno, P. G. Pagliuso, J. L. Sarrao, J. D. Thompson, E. A. Goremychkin, F. R. Trouw, M. P. Hehlen, and R. J. McQueeney, *Phys. Rev. B* **70**, 134505 (2004).